An immature, dedifferentiated, and lineage-deconstrained cone precursor origin of N-Myc initiated retinoblastoma

Hardeep P. Singh[a,b,c,*,1], Dominic W. H. Shayler [a,b] G. Esteban Fernandez[b], Matthew E. Thornton[d], Cheryl Mae Craft[c,e], Brendan H. Grubbs[d], and David Cobrinik[a,b,c,f,g,*]

[a] The Vision Center, Children's Hospital Los Angeles, Los Angeles, CA 90027

[b] The Saban Research Institute, Children's Hospital Los Angeles, Los Angeles, CA 90027

[c] USC Roski Eye Institute, Department of Ophthalmology, Keck School of Medicine, University of Southern California, Los Angeles, CA 90033

[d] Department of Obstetrics and Gynecology, Keck School of Medicine, University of Southern California, Los Angeles, CA 90033

[e] Department of Integrative Anatomical Sciences, Keck School of Medicine of the University of Southern California, Los Angeles, CA 90033, USA

[f] Department of Biochemistry & Molecular Medicine, Keck School of Medicine, University of Southern California, Los Angeles, CA 90033

[g] Norris Comprehensive Cancer Center, University of Southern California, Los Angeles, CA 90033

[*]Co-corresponding authors

Supporting Information Appendix

Supplementary Figures S1 – S9

Supplementary Table S1

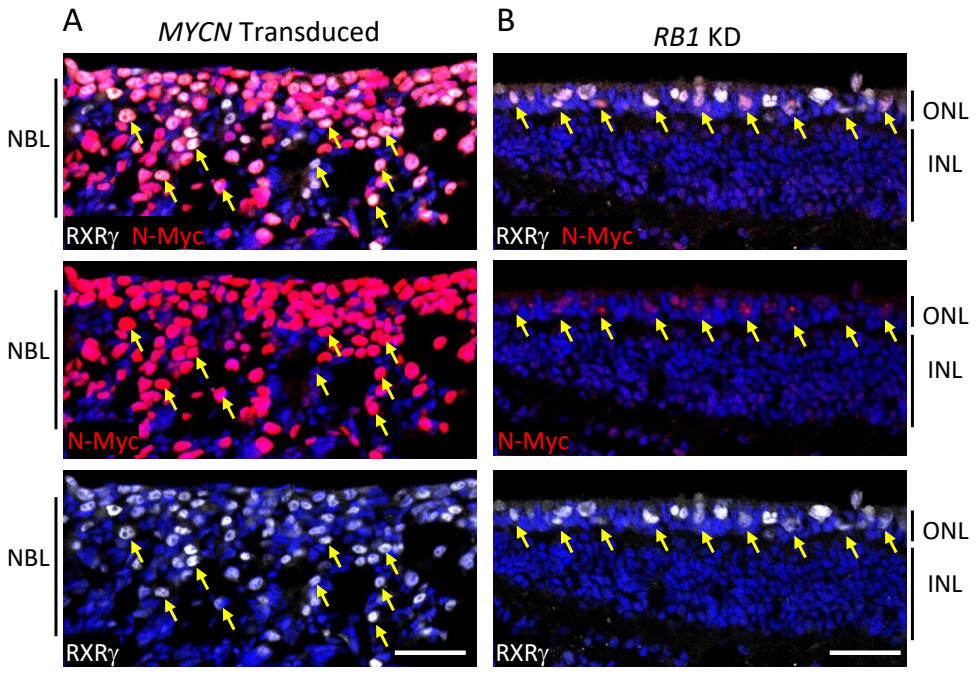

Figure S1. Higher N-Myc following *MYCN* transduction versus *RB1* knockdown. N-Myc immunostaining in retinal regions with many RXRγ^{+},Ki67^{+} cells at 14 days post *BE-MYCN* transduction (A) or 12 days post-infection with *RB1* knockdown construct pLKO.1C-sh*RB1* (18) (B). Cultured retinae were fixed and processed similarly and immunostained and imaged in parallel with identical settings. The neuroblastic layer (NBL), outer nuclear layer (ONL), and inner nuclear layer (INL) are indicated. Arrows, RXRγ^{+},N-Myc^{+} cells. Scale bars, 40 µm.

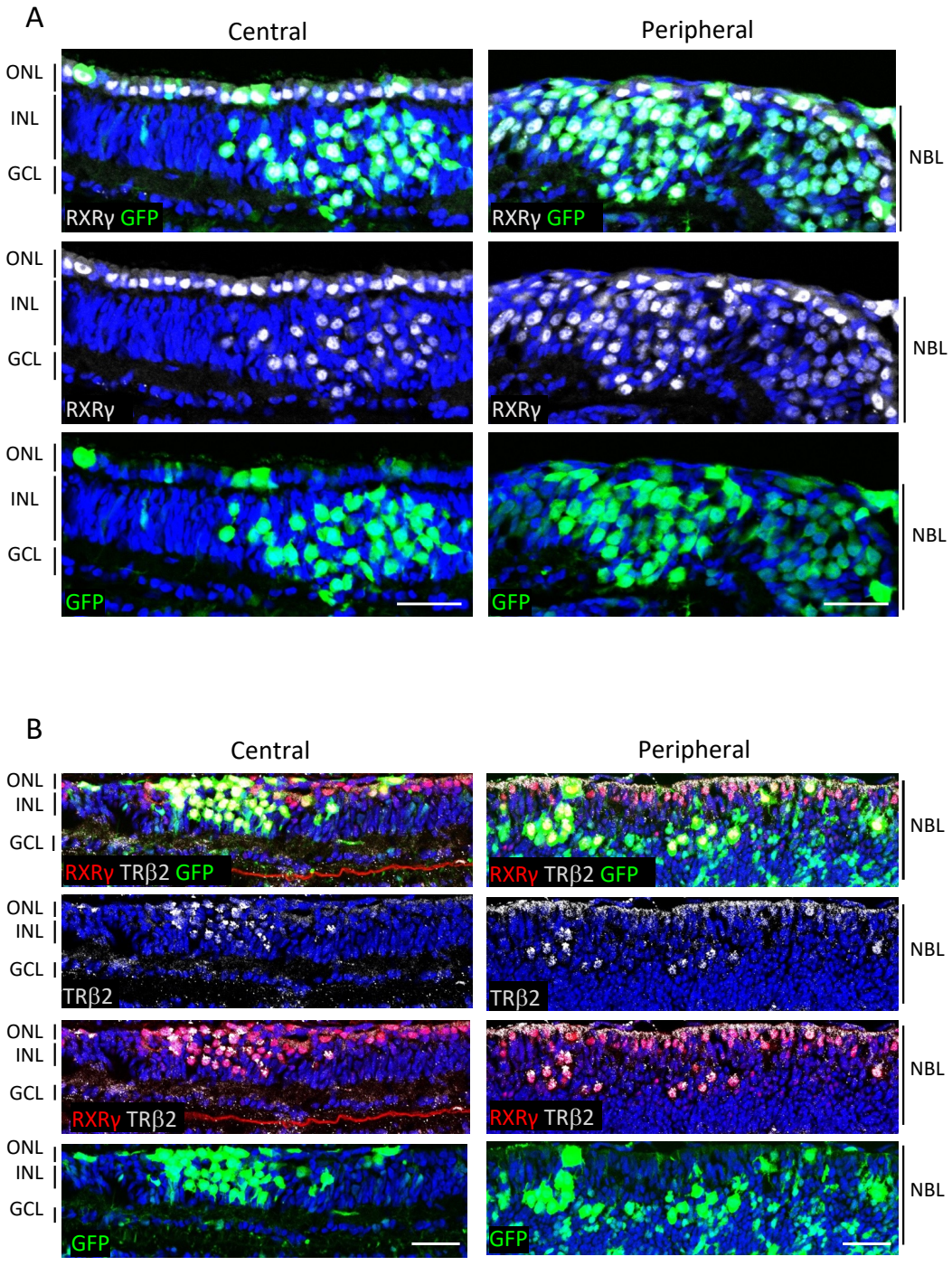

Figure S2. ***MYCN*-induced cone precursor foci in central and peripheral retina.** RXRγ (A) and RXRγ plus TRβ2 (**B**) immunostaining of foci in central and peripheral regions of the same explanted retina at 12 DIC after *BE-MYCN* transduction. GFP signal represents *BE-MYCN* transduced cells. Scale bars, 40 µm.

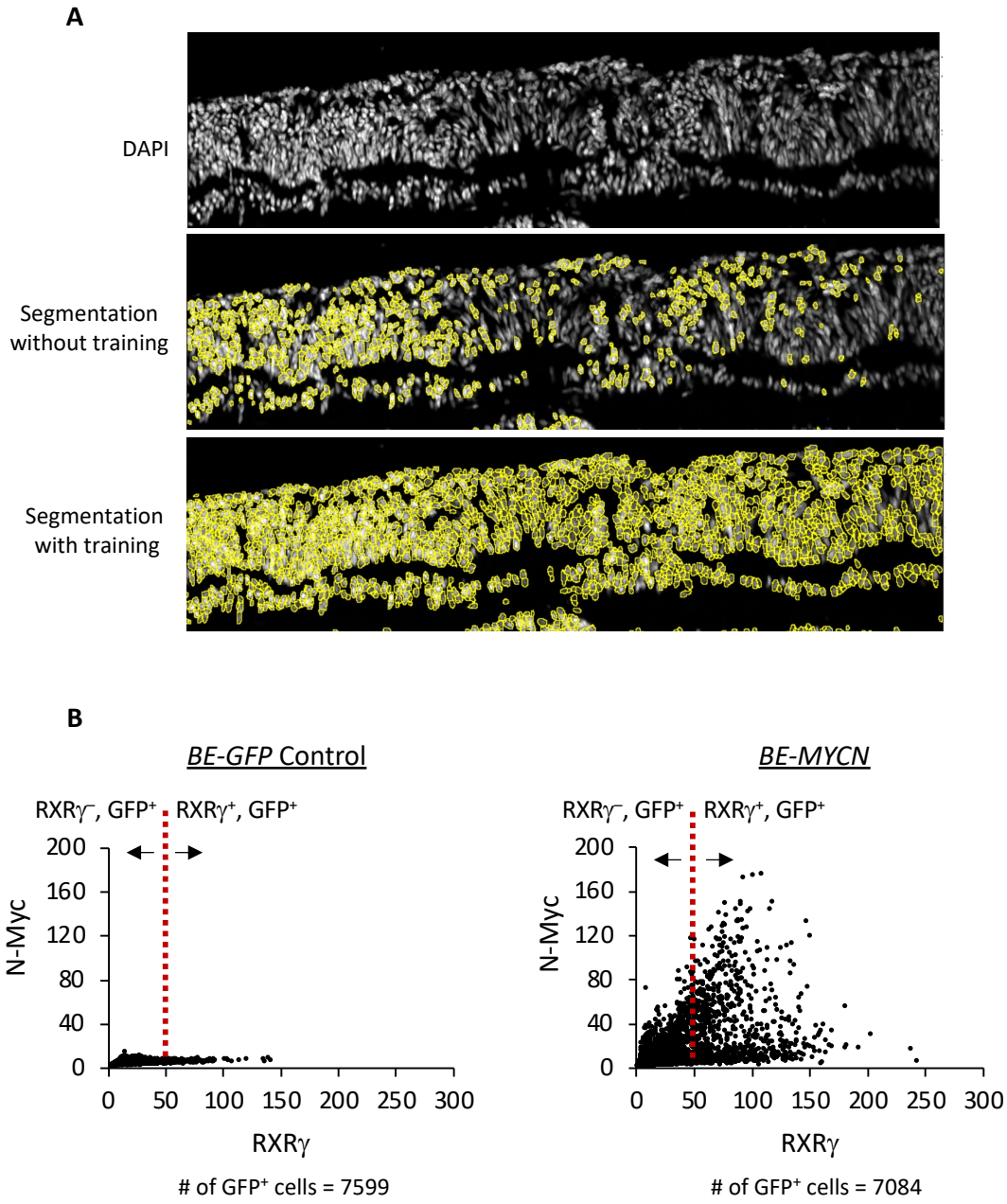

Figure S3. Trainable Weka based automated segmentation and single-cell quantitation of RXRγ and N-Myc expression. **A.** Representative region of a DAPI-stained explanted retina section segmented with and without WEKA based machine learning. **B.** Quantitation of N-Myc and RXRγ expression in 12 DIC retinae transduced with the *BE-GFP* control (*left*) or *BE-MYCN* (*right*) using WEKA and ImageJ. Retina section was co-stained for RXRγ, DAPI, and GFP as in Fig. 1C panels iii - iv. Red dotted line marks the threshold of RXRγ signal above background determined using a no-primary-antibody control. A plot of N-Myc levels in RXRγ$^+$ and RXRγ$^-$ cells based on this distribution is shown in Fig. 1F. Similar approaches were used to quantify co-immunostaining of Ki67 or RXRγ with different retinal markers.

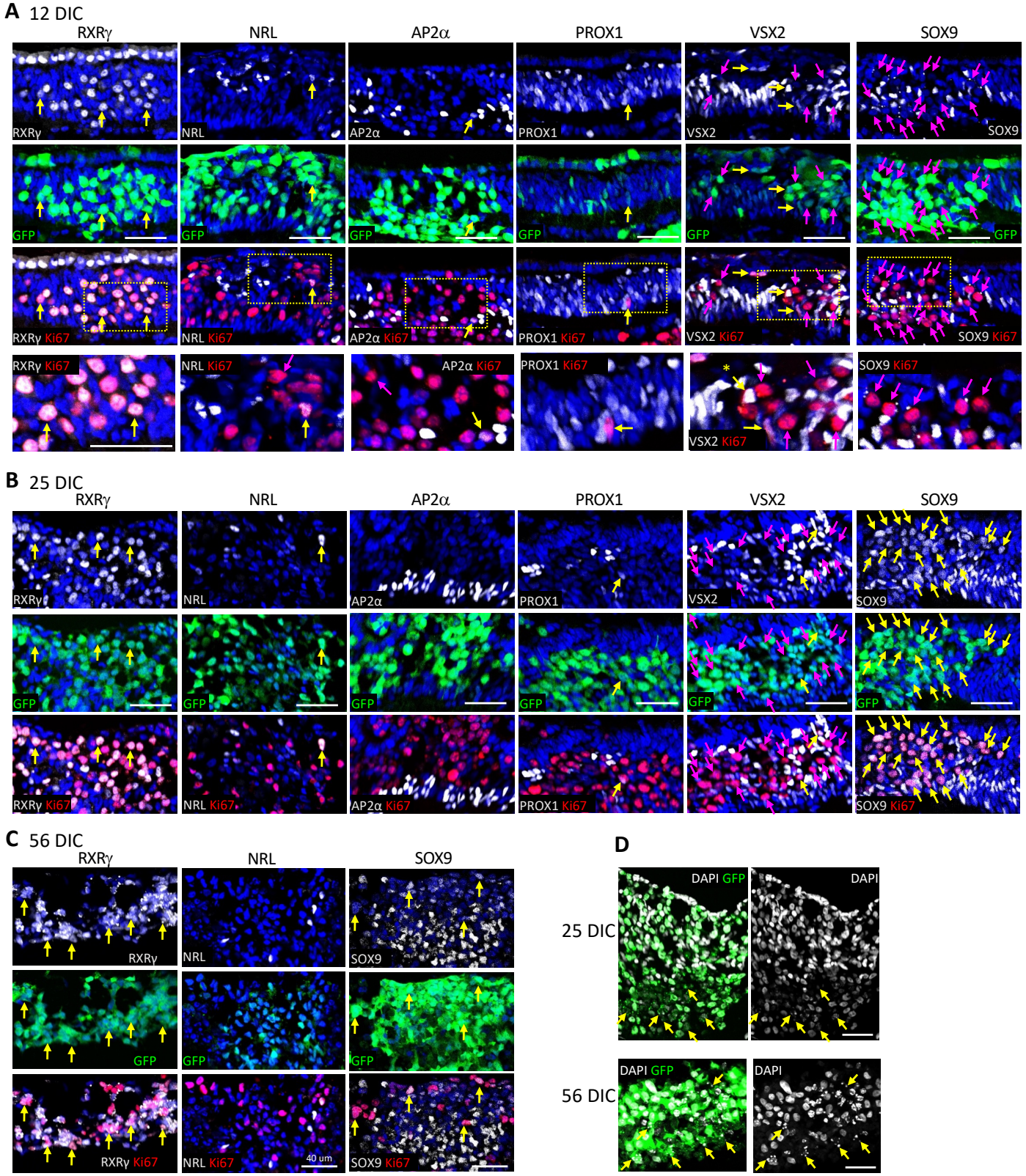
A 12 DIC
RXRγ
NRL
AP2α
PROX1
VSX2
SOX9
GFP
RXRγ Ki67
NRL Ki67
AP2α Ki67
PROX1 Ki67
VSX2 Ki67
SOX9 Ki67
B 25 DIC
C 56 DIC
40 um
D
25 DIC
56 DIC
DAPI GFP
DAPI

Figure S4. *MYCN*-induced cell cycle entry associated with expression of diverse retinal cell type markers. **A-C.** Representative co-immunostaining of Ki67 (red), the indicated retinal cell type markers (white), and GFP (green) in retinal explants at 12-, 25-, and 56-days post *BE-MYCN* transduction. Yellow arrows, transduced GFP^+,$marker^+$,$Ki67^+$. Pink arrows (for VSX2 and SOX9 staining), transduced GFP^+, $marker^-$, $Ki67^+$. **D.** At 25 and 56 DIC, many cells in GFP^+ foci had fragmented or undetectable nuclei (arrows) indicative of dead or dying cells. Scale bars, 40 μm.

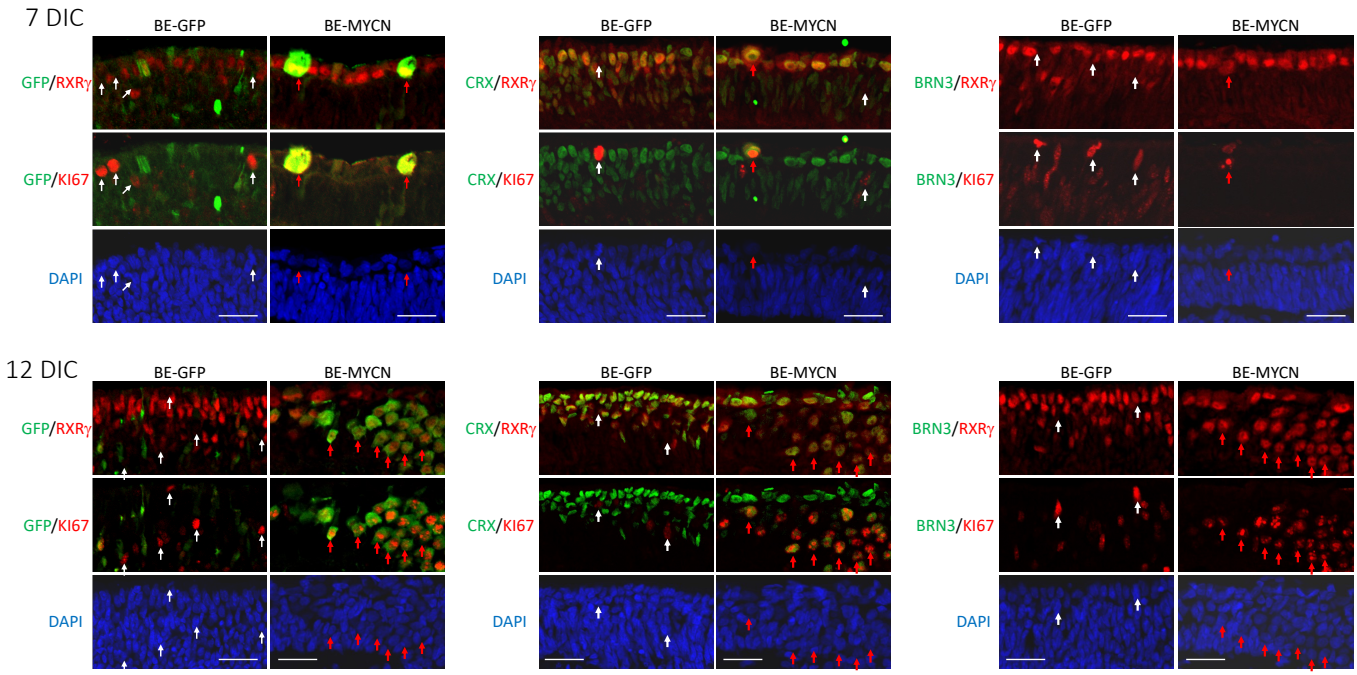

Figure S5. Expression of cone but not ganglion cell markers in initial *MYCN*-induced proliferating cells. Explanted retinae were transduced with *BE-GFP* or *BE-MYCN* and co-stained for GFP/RXRγ/Ki67 *(left),* CRX/RXRγ/Ki67 (*middle*), or BRN3/RXRγ/Ki67 (right) and cultured for 7 DIC (*top*) or 12 DIC (*bottom*). Two Ki67$^+$ populations were observed: White arrows*:* Ki67$^+$, RXRγ$^-$ cells (either GFP$^+$ or GFP$^-$) lacked CRX and BRN3, consistent with proliferating retinal progenitor cells in *BE-GFP* and *BE-MYCN* transduced retina. Red arrows: Ki67$^+$, RXRγ$^+$ cells were always GFP$^+$, CRX$^+$, and BRN3$^-$ and were seen only in *BE-MYCN*-transduced retina, consistent with MYCN-induced proliferating cone precursors. No BRN3$^+$ cells were detected in either retina at 7 or 12 DIC, consistent with retinal ganglion cell loss after optic nerve transection. (BRN3 staining positive control is shown in Fig. S6.) Scale bars, 25 μm.

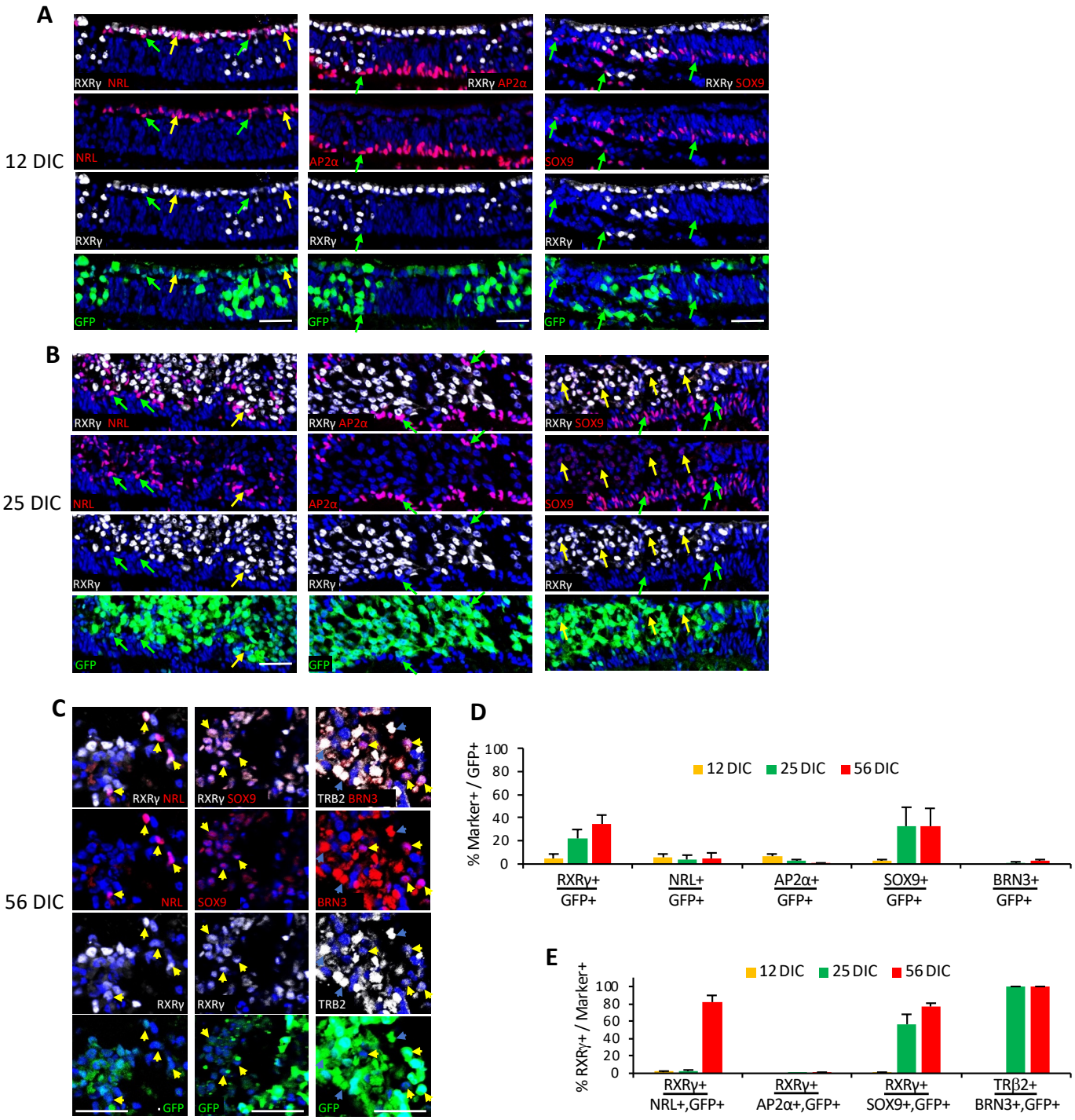

Fig. S6. Co-expression of cone markers with other cell type-specific markers in *BE-MYCN*-transduced retina. A-C. Co-staining of RXRγ or TRβ2 with NRL, AP2α, SOX9, or BRN3 at 12, 25, and 56 DIC following *BE-MYCN* transduction. Green arrows, cone marker-, other cell type marker$^+$; Yellow arrows, cone marker$^+$, other marker$^+$. Scale bars, 40 μm. **D-E.** Machine-learning based quantitation of the percent of transduced (GFP$^+$) cells expressing each marker (**D**) and the percent of the transduced marker$^+$ cells that co-expressed RXRγ or TRβ2 (**E**).

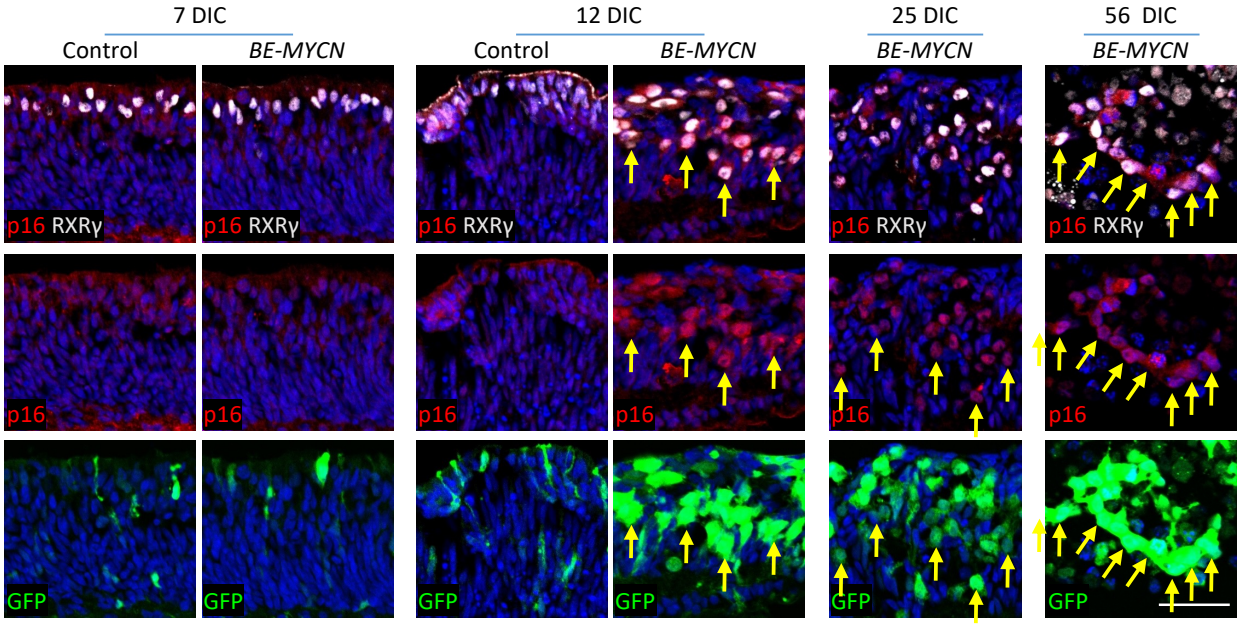

Fig. S7. *MYCN*-transduced cone precursors continuously over-express p16. Retinal explants at the indicated days post-infection with *BE-MYCN* or control *BE-GFP* vector and co-stained for p16 and RXRγ. Arrows, cells co-expressing p16, RXRγ, and GFP. Scale bar, 40 µm.

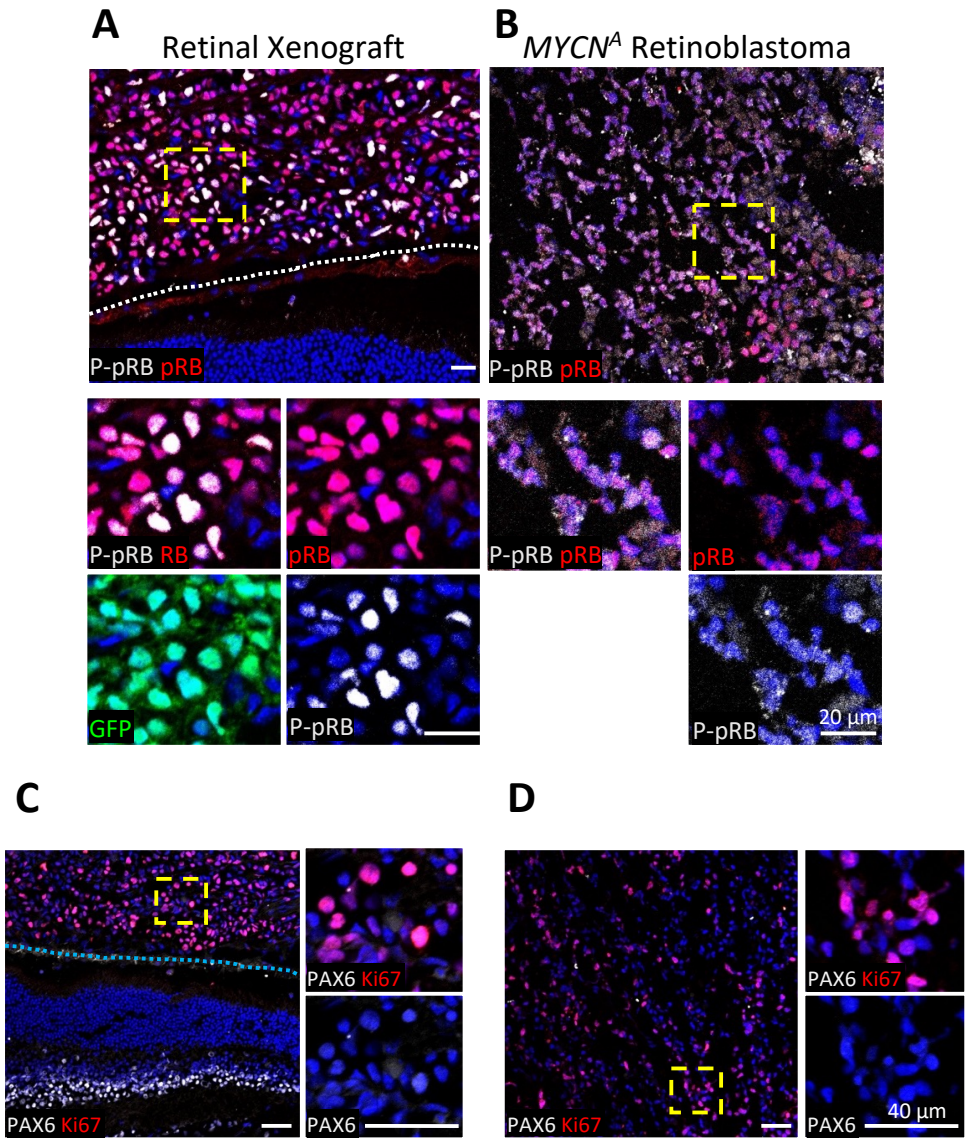

Fig. S8. Further characterization of MYCN-transduced retinal xenografts and *MYCNA* retinoblastoma. (**A-B**). pRB and p-pRB(S807, S811) co-expression in N-Myc overexpressing retinal xenografts (**A**) and a *MYCN*^{A} retinoblastoma (**B**). Scale bars, 20 µm. (**C-D**) Lack of detectable PAX6 in retinal xenografts (**C**) and *MYCN*^{A} retinoblastoma (**D**). Dashed boxes indicate regions shown in enlarged images. Scale bars, 40 µm.

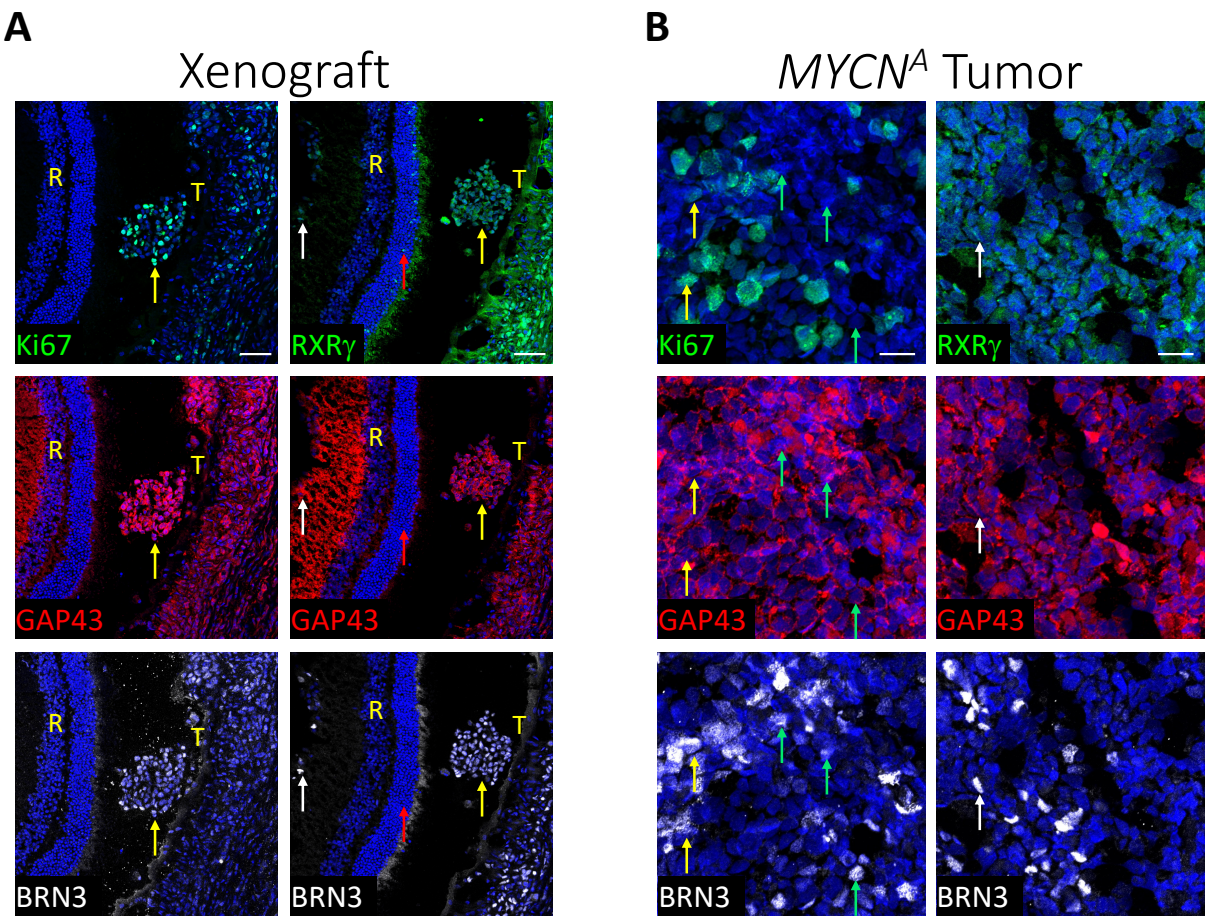

Figure S9. Co-expression of ganglion cell markers BRN3 and GAP43 in *MYCN*-transduced retinal xenografts and *MYCN*^{A} retinoblastoma tumors. A. *MYCN*-transduced retinal xenograft highlighting tumor (T) with widespread co-expression of Ki67, RXRγ, GAP43, and BRN3 (yellow arrows) and mouse retina (R) with RXRγ$^+$ but Ki67-, GAP43-, and BRN3-negative cones (red arrows) and RXRγ$^+$, GAP43$^+$, and BRN3$^+$ but Ki67-negative ganglion cells (white arrows). **B**. *MYCN*^{A} patient tumor was uniformly positive for GAP43 and RXRγ but inconsistently expressed BRN3. All BRN3$^+$ cells were GAP43$^+$ and RXRγ$^+$ (white arrows) while some were Ki67$^+$ (yellow arrows) and others Ki67$^-$ (green arrows). Scale bars, 50 μm (A), 25 μm (B).

Table S1. Antibodies used in this study.

Name	Clone	Species	Source	Catalog #	Titer
AP2α	3B5	Mouse	DSHB	3B5	1:20
ARR3 (LUMIf-hCAR)	-	Rabbit	Cheryl Craft (1)		1:5000
BRN3		Goat	Santa Cruz	sc-6026	1:50
CDK4	DCS-35	Mouse	Santa Cruz	sc-23896	1:50
CHX10 (VSX2)	-	Goat	Santa Cruz	sc-21690	2:200
CRX		Mouse	Abnova	H00001406-M02	
Cyclin D1	-	Rabbit	Millipore Sigma	ABE52	1:100
Cyclin D2	DCS-5	Mouse	Santa Cruz	sc-53637	1:50
Cyclin D3	D-7	Mouse	Santa Cruz	sc-6283	1:50
GAP43		Rabbit	Novus	NB300-143	1:1000
GFP	-	Goat	Abcam	ab6673	1:500
Ki67	B56	Mouse	BD Biosciences	550609	1:200
L/M-Opsin	-	Rabbit	Millipore	AB5405	1:500
Myc	9E10	Mouse	DSHB	9E10	1:1000
N-Myc	NCM II-100	Mouse	Santa Cruz	sc-56729	1:100
NRL		Goat	R&D Systems	AF2945	1:120
p16	-	Rabbit	Proteintech	10883-1-AP	1:100
Phospho-Rb (Ser807/811)	-	Rabbit	Cell Signaling	9308	1:1000
pRB	G3-245	Mouse	BD Biosciences	554136	1:100
PROX1	-	Rabbit	Angio-Bio	11-002	1:1000
RXRγ	-	Rabbit	Santa Cruz	sc-555	1:1000, 1:800
RXRγ	G-6	Mouse	Santa Cruz	sc-514134	1:200
SOX9	D8G8H	Rabbit	Cell Signaling Technol	82630	1:1000
TEAD4	1G7	Mouse	Developmental Studies Hybridoma Bank	PCRP-TEAD4	1:75
TRβ2	-	Rabbit	Santa Cruz	sc-67123	1:600

Supporting Information Reference:

1. A. Li, X. Zhu, B. Brown B, C.M. Craft, Gene expression networks underlying retinoic acid induced differentiation of human retinoblastoma cells. Invest. Ophthalmol. Vis. Sci. 44, 996-1007 (2003).